Catalysis Today 154 (2010) 46–52

Contents lists available at ScienceDirect

Catalysis Today

journal homepage: www.elsevier.com/locate/cattod

Ammonia oxidation on Ir(1 1 1): Why Ir is more selective to N_2 than Pt

C.J. Weststrate[b,*], J.W. Bakker[a], A.C. Gluhoi[a], W. Ludwig[c], B.E. Nieuwenhuys[a,b]

[a] Leiden Institute of Chemistry, Leiden University, P.O. Box 9502, Einsteinweg 55, 2333 CC Leiden, The Netherlands
[b] Schuit Institute of Catalysis, Eindhoven University of Technology, P.O. Box 513, 5600 MB Eindhoven, The Netherlands
[c] Fritz-Haber-Institut der Max-Planck-Gesellschaft, Faradayweg 4–6, 14195 Berlin, Germany

ARTICLE INFO

Article history:
Available online 21 April 2010

PACS:
82.45.Jn
82.75.+r
82.80.Pv

Keywords:
Ammonia
Iridium
Ir(1 1 1)
Ammonia adsorption
Ammonia decomposition
Ammonia oxidation

ABSTRACT

NH_3 does not dissociate on a clean Ir(1 1 1) surface, but dissociation can be induced by radiation, which yields all possible NH_{xad} species. NH_{ad} is the most stable and it is the only intermediate found at room temperature. NH_{ad} decomposes between 350 and 500 K, yielding NH_3 (g) and N_{ad}, which desorbs as N_2 between 550 and 700 K. Adsorbed oxygen atoms induce NH_3 dissociation between 300 and 400 K, forming NH_{ad} and H_2O. NH_{ad} decomposes further between 350 and 450 K, forming N_{ad} and H_2O. Measurements of the surface composition during ammonia oxidation showed a mismatch between the change of the surface coverage (from N_{ad} to O_{ad}-dominated) and that in the gas phase (from N_2 to NO). This is explained by a higher barrier for NO (g) formation as compared to N_2 formation on Ir(1 1 1). On Pt(1 1 1) the difference in barrier height for N_2 vs. NO formation is smaller, which explains why Pt is more selective to NO than Ir.

1. Introduction

Ammonia is formed as an unwanted side product in several industrial processes. The removal of ammonia can be achieved in a selective catalytic reaction between NH_3 and O_2. The desired products in this case are N_2 and H_2O. A catalyst for this process needs to be both active and selective towards N_2 rather than NO_x. Ir based catalysts show the desired activity and selectivity [1]. Catalytic oxidation of NH_3 on Ir has been studied before by several authors, both for high surface area catalysts and single crystal surfaces [1–8]. In previous publications we reported on NH_3 decomposition and oxidation on Ir(1 1 0) [4–8] and a model was proposed to explain the selectivity towards N_2 instead of NO [8] for this particular Ir surface. The (1 1 0) surface shows 'special' behavior in the sense that N_2 formation on this surface is accelerated by the presence of O_{ad} due to repulsive interactions between O_{ad} and N_{ad} [7,9]. The (1 1 1) surface, which is usually the most common plane on small catalyst particles, is a more representative candidate to be used as a model to study the behavior of Ir catalysts. We already published some desorption spectra and temperature programmed reaction data that were obtained on the Ir(1 1 1) surface [8]. The present paper describes new results that were obtained on Ir(1 1 1) using high resolution, fast XPS, which gives information about the nature and concentration of adsorbates *during* a catalytic reaction. A similar study was reported for Pt(1 1 1) by Mieher and Ho [10], who used thermal desorption and EELS to study O_{ad}-induced NH_3 decomposition. Although there are many more surface science studies concerning NH_3 oxidation, on various surfaces (Cu [11], Ru [12], Ag [13], Ni [14] and Rh [15]), we limit the discussion here to Ir and compare it to Pt (used as a catalyst in the Ostwald process [16] to make NO_x from NH_3), two metals that show different selectivity in the NH_3 oxidation reaction.

2. Experimental

The vacuum systems used for the TPD and XPS measurements (performed at the SuperESCA beamline of ELETTRA, the synchrotron radiation facility in Trieste, Italy) are described in detail elsewhere [7]. The pressures reported here are uncorrected ion gauge readings. The Ir single crystal (diam. 1 cm, thickness 2 mm) was cut and polished to within 0.1° of the desired (1 1 1) orientation. It was cleaned using Ar^+ sputtering and annealing (1400 K) cycles, followed by oxygen treatments. The oxygen was removed either by flashing to 1400 K or by heating in the presence of hydrogen. In the latter case, H_2 was removed by a final flash to 700 K. The cleanliness of the sample was checked by XPS, showing no oxygen and carbon contamination. The N1s spectra were measured with a photon energy of 480 eV, for the O1s spectra a photon energy of 650 eV was

* Corresponding author.
E-mail address: c.j.weststrate@tue.nl (C.J. Weststrate).

0920-5861/$ – see front matter © 2010 Elsevier B.V. All rights reserved.
doi:10.1016/j.cattod.2010.03.049

used. Temperature programmed XPS (TP-XPS) measurements were performed using heating rates between 0.3 and 0.65 K s^{-1}. The different core level regions were measured in a separate experiment, i.e. during one experiment either O1s or N1s could be measured. The XP spectra were evaluated, after subtraction of a linear background, by fitting the peaks with a Doniach–Šunjić lineshape convoluted with a Gaussian function [17] to account for experimental and thermal broadening. The binding energy (BE) values are reported here with respect to the Fermi level, measured using the same excitation energy that was used to measure the spectra.

Quantification of the O1s signal intensity was done using an oxygen-saturated surface as a reference, prepared by dosing O_2 at 300 K. Earlier studies report a saturation coverage of 0.5 ML, based on the (2×2) LEED pattern observed after dosing O_2 at room temperature [18–21]. Recently, the adsorption of oxygen was studied using XPS, and a saturation coverage of 0.38 ML was reported [22]. This value was used to calibrate the oxygen coverage in our experiments. Quantification of the N1s spectra was more complicated and was done indirectly. In an experiment where O_{ad} reacted with NH_{3ad} to form N_{ad} (discussed in detail in 3.2) the decrease of the O_{ad} signal was used to calculate the N_{ad} coverage based on the stoichiometry of the reaction.

In our earlier XPS studies beam-induced NH_{3ad} dissociation was observed [6]. In experiments where we wanted to keep the beam damage as low as possible, the steps preceding the actual measurements were preformed in the absence of radiation and the heating rate was doubled, so that the experiment would be faster and thus, the beam damage would be minimized. The sample position was also regularly changed to check that the areas which had not been exposed to the beam showed the same changes. In this way, we ensured that the data reported here do not suffer from beam damage.

In the study presented here, beam damage was used as a tool to create NH_{xad} species on the surface and to study their thermal behavior. The beam flux on the sample is typically 10^{11} to 10^{13} photons s^{-1}, depending on the settings of the exit slit and the photon energy. The spot size is determined by the size of the exit slit of the monochromator, which was chosen such that the beam spot on the sample is between ~1 and 2 mm in our experiment. The beam damage in the XPS experiment is thought to be primarily due to the photoelectrons generated by the X-rays, rather than a direct X-ray induced process. This is confirmed by the fact that NH_{3ad} dissociation was also found after irradiation with 60 eV electrons. The latter method was used to obtain temperature programmed desorption (TPD) results and has been used before by other authors who studied surfaces on which NH_{3ad}, like on Ir(1 1 1) [8,23], does not dissociate [13,24–26]. Since we use beam damage here merely as a tool, to study the thermal behavior of NH_{xad} species, the beam damage process will not be discussed in more detail here.

3. Results and discussion

Fig. 1 shows schematically how the different N1s components found throughout the experiments were assigned to the different NH_{xad} species, by careful comparison with thermal desorption experiments. The binding energy of NH_{3ad} was determined by adsorption of NH_3 at 100 K followed by heating to 220 K. The binding energy of N_{ad} was established by heating a co-adsorbed O_{ad}/NH_{3ad} layer. Above 400 K one N1s species exists, which desorbs as N_2 (discussed in detail in Section 3.2). It should be noted here that the BE value of N_{ad} is sensitive to the chemical environment of the N_{ad}, and shifts of ~0.3 eV were seen during the experiments. During heating of a beam-damaged NH_{xad} layer, a single species exists on the surface between 300 and 400 K, which decomposes into N_{ad} between 400 and 500 K. On Ir(1 1 0) a species with a very

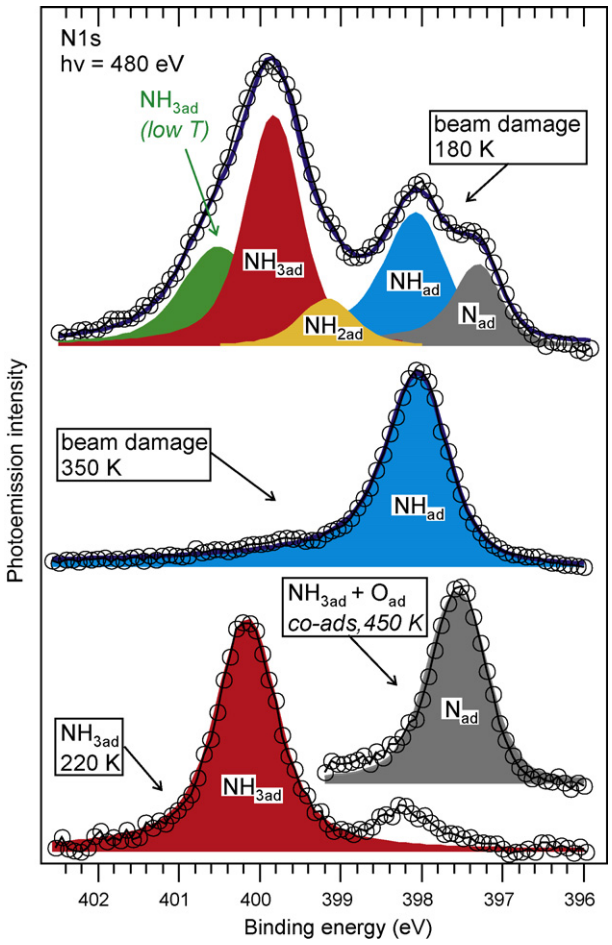

Fig. 1. N1s spectra taken during different experiments, illustrating how the peak shape and binding energy for the different NH_{xad} species was determined. See text for details. The experimental points are represented by open circles, while the fitting result is indicated by a solid line.

similar binding energy and similar thermal behavior was identified as NH_{ad}. Thus, the same assignment was used here [6]. The spectral shapes and binding energies of the afore mentioned species were used to analyze the composition of the mixture of NH_{xad} species existing on the surface at 180 K after beam-induced decomposition has occurred. The NH_{3ad} BE value is affected by the chemical environment of the NH_{3ad}, especially in the low temperature regime, where the presence of another NH_{3ad} species (top spectrum) causes a downward shift of ~0.3 eV as compared to the spectrum where only one NH_{3ad} species is present. Next to the already identified species, two other components had to be used to properly fit the spectrum. One component with a BE of 399.2 eV was assigned to NH_{2ad}, based on its BE value which is just between that of NH_{3ad} and NH_{ad}. Another component at the high binding energy side was assigned to another adsorbed NH_3 species present only at low temperatures. In the present article, we limit the discussion on the NH_3 surface chemistry to the temperature regime above 200 K, where only one form of chemisorbed NH_3 is present. A more detailed discussion on low temperature adsorption states of NH_3 on various substrates can be found in Ref. [6] and references therein. For the O1s region only one species, assigned to O_{ad}, was applied to fit the O1s spectra for all experimental conditions. Other possible O-containing species, such as NO and H_2O, would appear at significantly different binding energies and would be easily distinguished (see Table 1).

The binding energy values that were found on Ir(1 1 1) are summarized in Table 1, together with values found earlier on Ir(1 1 0).

Table 1
Binding energies (eV) for nitrogen and oxygen species found during ammonia oxidation on Ir(1 1 1) and Ir(1 1 0) [6,7]. Note that the O1s BE values reported in Ref. [7] were off by ~0.5 eV. In this table the correct values for these O1s species on Ir(1 1 0) are reported, with respect to the Fermi edge.

Species	N1s, Ir(1 1 1)	N1s, Ir(1 1 0)	O1s, Ir(1 1 1)	O1s, Ir(1 1 0)
NH_{3ad}	399.8–400.1	400.2	–	–
NH_{2ad}	399.2	–	–	–
NH_{ad}	398.1	398.3	–	–
N_{ad}	397.3–397.6	397.2	–	–
O_{ad}	–	–	530.0	529.9
NO_{ad}	Not obs.	400.5	Not obs.	532.5
H_2O	–	–	Not obs.	532.2

For the BE values reported in Refs. [6,7] an incorrect value for the Fermi edge was used, resulting in a consequent deviation of 0.7 eV (N1s) and 0.5 eV (O1s) from the correct values. This data has been revisited using a proper Fermi edge correction and the correct BE values for Ir(1 1 0) are shown in Table 1. The values found for Ir(1 1 0) and Ir(1 1 1) are in excellent agreement. The differences in BE that exist between this study and those reported for NO on Ir(1 1 0) by de Wolf et al. [9,27] are most probably due to the fact that in those studies Ir photoemission peaks were used for BE calibration, instead of the Fermi edge as used in the present study.

3.1. NH_{xad} surface chemistry

Fig. 2 shows the results of two experiments in which an adsorbed NH_3 layer (saturation, 5 L) was heated. The process was followed by TPD and by TP-XPS. In the first experiment (shown left), radiation damage was kept to the minimum. In the second experiment (shown right), beam damage was intentionally created before the heating was started.[1] In the absence of beam damage, NH_3 desorbs molecularly in a broad temperature region between 100 and 400 K [8]. Panel (a) only shows the temperature region that matches the TP-XPS data. The inset shows the full desorption trace, including the physisorbed states present below 150 K (discussed in detail elsewhere, see for example Ref. [6]). In the corresponding TP-XPS experiment, NH_{ad} slowly builds up due to beam damage. This shows that beam damage, although present, is a slow process, and it can easily be distinguished from the real chemistry.

At 200 K the irradiated NH_{3ad} layer (Fig. 2, righthand side) contains all possible NH_{xad} species, in different concentrations. NH_{2ad} decomposes around 230 K (into NH_{ad}) and NH_{3ad} desorbs molecularly between 200 and 350 K. The atomic nitrogen that was initially present disappears around 300 K, but not due to desorption of N_2. The decrease of the N_{ad} is assigned to hydrogenation of N_{ad} into NH_{ad}. On Ir(1 1 0) it was shown before that N_{ad} can be hydrogenated below 300 K [6]. This shows that NH_{ad} is the most stable NH_{xad} species and that conversion of NH_{2ad} and N_{ad} (in the presence of H_{ad}) to NH_{ad} readily occurs around or below room temperature. The NH_{ad} concentration increases between 200 and 400 K, reaching a maximum of ~0.23 ML. It is interesting to note here that a (2×2) LEED pattern could be generated [shown in the inset of Fig. 2(d)] when the Ir(1 1 1) sample was exposed to NH_3 at 300 K and irradiated with 60 eV electrons. We tentatively assign this to a $p(2 \times 2)$ overlayer of NH_{ad} on the sample, with a coverage of ~0.25 ML, in line with the NH_{ad} coverage found by XPS at ~300 K. On Pt(1 1 1) NH_{ad} was also found to be the most stable NH_{xad} species in experiments where an NH_{3ad} layer was irradiated and heated [24]. Hydrogenation of N_{ad} to NH_{ad} on Pt(1 1 1) also occurs between 200 and 300 K [25].

NH_{ad} decomposes between 360 and 530 K, forming 0.1 ML of N_{ad} and releasing 0.13 ML 'N' into the vacuum. The TPD experiment [Fig. 2(b)], gives some information on the desorbing products around this temperature. The most obvious candidate is N_2, and this is indeed observed at these temperatures in the gas phase during TPD. A detailed analysis of the TPD result reveals that desorption of N_2 is not the only pathway. First of all, the NH_3 desorption peak between 380 and 500 K is not observed when there is no beam damage. This suggests that it is due to NH_3 formation at this temperature by hydrogenation of NH_{ad}. In such a reaction three NH_{ad} species are needed to generate one NH_3 molecule, and two N_{ad} species are formed (Eq. (1)). The H_2 desorption trace presents further evidence for such a reaction: the desorption peaks below 350 K are due to combination of H_{ad}[28], formed during (radiation-induced) NH_{3ad} decomposition, while the desorption peak between 440 and 590 K is due to decomposition of NH_{ad}. The latter peak is much smaller than what would be expected when decomposition of NH_{ad} into N_{ad} and H_2 is the only mechanism (peak ratio 2:1). We suggest the following mechanisms during NH_{ad} decomposition: at the onset of NH_{ad} decomposition (Eq. (2)) some N_{ad} and H_{ad} are created, while the NH_{ad} concentration is still high. Free H_{ad} on the surface combines to H_2 (g) below 350 K [28], so that any hydrogen formed > 400 K will have a short residence time. It is, however, just enough for hydrogenation of NH_{ad}, forming ultimately NH_3, which desorbs upon formation (Eq. (3)). At higher temperatures, the NH_{ad} concentration has decreased and molecular hydrogen desorption is favored over NH_{ad} hydrogenation. The N_{ad} formed after NH_{ad} decomposition desorbs as N_2 between 400 and 700 K.

$$3\,NH_{ad} \rightarrow 2\,N_{ad} + NH_3(g) \quad (1)$$

$$NH_{ad} \rightarrow N_{ad} + H_{ad} \quad (2)$$

$$NH_{ad} + 2\,H_{ad} \rightarrow NH_3(g) \quad (3)$$

3.2. Influence of O_{ad} on NH_{3ad} decomposition

The influence of O_{ad} on the NH_{xad} chemistry was studied in an experiment in which an O_{ad} covered surface (0.38 ML) was exposed to NH_3 (5 L, 150 K) and heated afterwards. The results are shown in Fig. 3. In the TPD experiment, the H_2O desorption trace displays four different peak maxima between 150 and 400 K. On the basis of our XPS results the different peaks can be attributed to different surface reactions. The H_2O desorption around 190 K corresponds to the desorption temperature of adsorbed H_2O (see supplementary information, Fig. S1). It is therefore tentatively assigned to water that was adsorbed from the background gas or a small H_2O contamination in the NH_3 used for the TPD experiments. In the XPS experiment, however, the O1s spectra did not reveal any adsorbed water. It could also correspond to a low temperature reaction between O_{ad} and NH_3. Evidence for such a reaction can be found in the presence of NH_{2ad} already at the onset of the XPS measurement. The peak at 220 K is accompanied by decomposition of NH_{2ad} into NH_{ad}. All these low temperature processes cause only a minor decrease of the O_{ad} concentration and might be influenced by beam damage. The most obvious influence of O_{ad} is seen above 280 K, where the TP-XPS data shows reaction of NH_{3ad} to NH_{ad}, which starts at 280 K. It is accompanied by a significant O_{ad} consumption and a H_2O desorption peak. At 350 K the NH_{ad} concentration reaches a maximum of 0.05 ML, after which it decreases. This decrease is accompanied by a fast increase of the N_{ad} concentration, O_{ad} consumption, a H_2O desorption peak (400 K) and the

[1] For the TPD experiment the adsorbed NH_3 layer was exposed to 60 eV electrons, for ~5 min. In the TP-XPS experiment the exposure to 480 eV X-rays (used to measure the N1s level) was 25 min. before the measurement was started. Our TP-XPS results show that TPD and XPS can be safely compared: The only possible products that beam-induced dissociation can yield are NH_{2ad}, NH_{ad} and N_{ad}, irrespective of the type of radiation used. During TP-XPS both NH_{2ad} and N_{ad} were found to be converted into NH_{ad}. It is therefore very likely that a similar process would yield an NH_{ad}-covered surface at 300 K after electron-beam-induced damage.

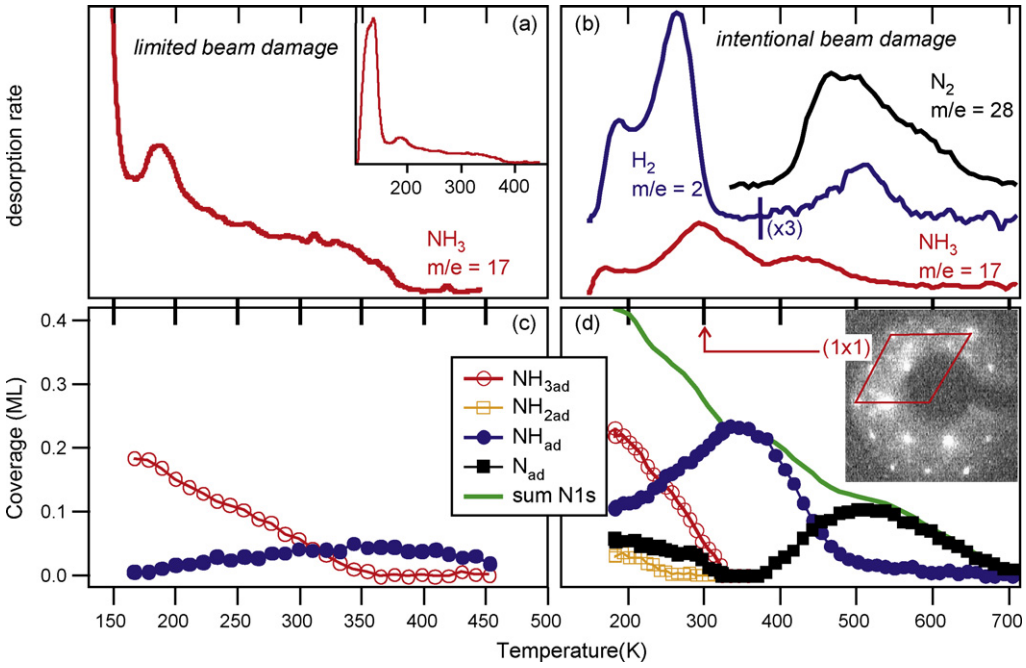

Fig. 2. (a) TPD (0.4 K s^{-1}) NH_3 desorbs molecularly, between 100 and 400 K. The main panel shows a zoom-in of the temperature region that matches the XPS data. The inset shows the desorption spectrum of the surface after saturation with NH_3. (c) TP-XPS, (0.65 K s^{-1}) of an adsorbed NH_3 layer. The slow build-up of NH_{ad} is due to radiation-induced dissociation. (b) TPD (3 K s^{-1}) of an irradiated NH_{3ad} layer, showing desorption of N_2 and H_2, decomposition products of NH_3. Note that the H_2 trace > 400 K is multiplied by 3. (d) TP-XPS (0.5 K s^{-1}) after beam-induced dissociation of an NH_{3ad} layer, showing the formation of various NH_{xad} species and their thermal behavior during heating. The inset of panel (d) shows a (2 × 2) LEED pattern, observed after irradiation (60 eV electrons), during NH_3 dosing at 300 K. It is tentatively assigned to a p(2 × 2)-NH_{ad} layer with a coverage of ~0.25 ML.

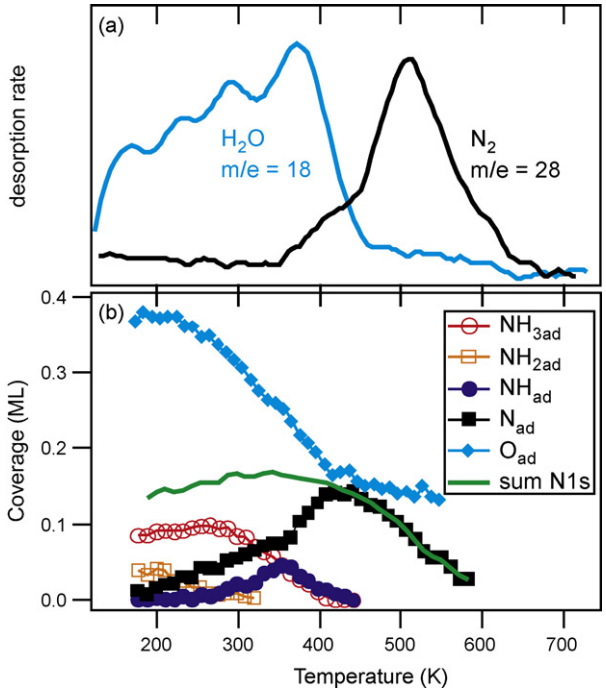

Fig. 3. TPD (1 K s^{-1}) and TP-XPS (0.65 K s^{-1}) after saturation (0.38 ML O_{ad}) with O_2 at 300 K and 5 L NH_3 (150 K). Panel (a) shows that H_2O desorbs in four different peaks, between 150 and 400 K. N_2 desorbs between 450 and 650 K. Hydrogen adsorption was not found at all. Panel (b) shows the corresponding TP-XPS results, showing the O-assisted decomposition of NH_{3ad} to NH_{ad} between 300 and 450 K and O-assisted NH_{ad} decomposition into N_{ad} between 350 and 450 K.

onset of N_2 (g) formation, i.e., at this temperature NH_{ad} reacts with O_{ad} to N_{ad}, H_2O (g) and some N_2 (g). We cannot completely exclude that N_{ad} formed between 200 and 350 K is due to beam-induced dissociation. We therefore do not interpret this in detail and limit the discussion here to N_{ad} formation above 350 K that is more obviously due to surface chemistry, as corroborated by the TPD where beam damage was absent. NH_{ad} decomposition in the presence of O_{ad} occurs at a significantly lower temperature than NH_{ad} decomposition in the absence of O_{ad}, i.e. NH_{ad} dehydrogenation is assisted by atomic oxygen, similar to what was found on Ir(1 1 0) [7]. At 420 K all NH_{xad} is converted into N_{ad}, and the O_{ad} concentration stabilizes at ~0.15 ML. The further slow decrease of the O_{ad} signal is assigned to reactions with background gases such as H_2 and CO. The N_2 desorption temperature is not affected very much by the presence of O_{ad}, in contrast to the strong downward shift found on Ir(1 1 0) [4,7,27,29].

The role of oxygen in NH_3 dissociation can be described in two ways, either via a direct reaction between O_{ad} and NH_{3ad}, or by an indirect influence of the oxygen. The adsorption of oxygen influences the reactivity of the metal surface and can thereby indirectly enhance NH_3 decomposition [30]. The latter model was used to explain oxygen-enhanced dissociation of NH_{3ad} on Ir(1 0 0) [3]. In their experiments water formation was not found, the only products being H_2 and N_2, which excludes the direct reaction between adsorbates. In our experiments water formation is found while hydrogen desorption is absent. We can therefore not distinguish between the two models.

The formation of NO_{ad}, NO (g) or N_2O (g) was not observed on Ir(1 1 1), not even during an experiment in which a mixed NH_{3ad}/O_{ad} layer was heated in the presence of O_2 (g) (see supporting information, Fig. S2). This is in contrast to our findings on Ir(1 1 0), where NO_{ad} formation was found when O_{ad} and N_{ad} were both present above 400 K. On Ir(1 1 1) all the 'ingredients' to form NO_{ad} are present on the surface, i.e. NH_{ad} and O_{ad} co-exist on the surface between 300 and 400 K and N_{ad} and O_{ad} co-exist on the surface between 200 and 500 K. This is due to the fact that the dissociated state is more stable than NO_{ad} on Ir(1 1 1), i.e. there is no thermodynamic driving force towards NO formation (see also the discussion in Section 3.4).

3.3. Temperature programmed ammonia oxidation

The gas phase products found during temperature programmed NH_3 oxidation on Ir(1 1 1) have been reported briefly in Ref. [8], for three different reactant ratios. In the present study we report new results obtained using a combination of TP-XPS to determine the nature and concentration of the surface species and measurements of the gas phase composition during temperature programmed ammonia oxidation. Fig. 4 shows the results for NH_3/O_2 ratios of 1:1 and 1:4. A more comprehensive TPR study for different reactant ratios and absolute pressures can be found in supporting information, Fig. S3. From the data presented there, it becomes clear that the absolute pressure only affects the reaction rate, not the temperature where the gas phase selectivity changes from N_2 to NO. This fact allows us to safely compare the TPR and TP-XPS data shown in Fig. 4, even though the reactant pressures differ by one order of magnitude.

3.3.1. Ratio 1:1

The XPS measurements were done in the following way: first the surface was exposed to NH_3 (5×10^{-8} mbar) and subsequently the oxygen pressure was established. The dissociative adsorption of O_2 is partially inhibited by the presence of NH_{3ad} resulting in an O_{ad} coverage of only 0.16 ML (40% of saturation coverage) at the beginning of the heating. The behavior of the surface species in this experiment is similar to what was observed for a mixed NH_{3ad}/O_{ad} overlayer, i.e., formation of NH_{ad} around 300 K and formation of N_{ad} around 400 K (Fig. 3). From XPS it can be seen that N_{ad} accumulates on the surface, while the equilibrium O_{ad} concentration is almost zero. However, O_2 adsorption/decomposition still occurs, as evidenced by the gas phase, showing continuous N_2 formation for $T > 400$ K. Above 500 K the surface composition changes and N_{ad} is gradually replaced by O_{ad}. Up to 650 K, the O_{ad} concentration rapidly increases up to 0.11 ML (at 650 K), while further heating only results in a very slow increase. Formation of NO_{ad} was not observed in this experiment. It is important to note that the change of gas phase selectivity to N_2 occurs 80 K higher than the change of surface composition. This means that N_2 is the only gas phase product at 600 K, even though the surface concentrations of N_{ad} and O_{ad} at this temperature are equally large.

3.3.2. Ratio 1:4

A change of the gas phase reactant ratio from 1:1 to 1:4 does not affect the low temperature NH_3 + O_{ad} surface chemistry. At 400 K, at the onset of the reaction, the surface is covered with N_{ad} (0.27 ML) and the O_{ad} concentration is very low. In a separate experiment where the reaction (ratio 1:4) was stopped around 400 K, the reactants were pumped away, and the surface was cooled to 250 K, a (2×2) LEED pattern was visible [shown in the inset of panel (b)]. It is assigned to a p(2 × 2)-N_{ad} structure with a coverage of ~0.25 ML, in line with the N_{ad} coverage determined by XPS. The most important influence of the higher O_2 partial pressure on the surface composition is observed around 500 K, where the change of surface composition from N_{ad} to O_{ad} occurs faster and at a lower temperature than for the 1:1 ratio. A maximum O_{ad} concentration of 0.23 ML is reached, about twice the amount found for the 1:1 ratio. For the higher O_2 partial pressure, both the surface composition and the gas phase selectivity change at lower temperatures, but the T-difference between surface composition change and gas phase selectivity change is ~80 K, for both reactant ratios.

3.4. Comparison between Pt and Ir: understanding selectivity

Platinum and iridium show significantly different catalytic properties when used as a catalyst for ammonia oxidation [1]. In this section we discuss the differences and propose an explanation for this based on the adsorption energies of the adsorbates on the surface.

Ammonia dissociates on more open Ir surfaces, such as Ir(1 1 0) and Ir(5 1 0) [6,5], but not on the smooth, close-packed (1 1 1) surface [23]. A slightly sputtered (1 1 1) surface is also active for NH_3 dissociation [8], showing that the dissociation activity is related to the presence of low-coordinated Ir atoms (defects). On Pt, on the other hand, defects do not help to dissociate NH_3 at low temperature [26,31,32], although NH_3 dissociation was observed in the presence of NH_3 (g) above 400 K [33,34].

For both metals O_{ad} has a beneficial effect on NH_{3ad} decomposition: on Pt it is essential for low temperature dissociation [10,31,35], on Ir it is essential to dissociate NH_{3ad} on the close-packed (1 1 1) surface, and it lowers the NH_{ad} decomposition temperature on several Ir surfaces [7]. On Ir(1 1 0) it also lowers the temperature for N_{ad} combination to N_2 (g) [6]. The most pronounced difference between Pt and Ir is found during temperature programmed ammonia oxidation. On Pt surfaces, formation of NO_{ad} occurs readily, even at 250 K [26,35,36], and NO is the dominant product of the ammonia oxidation reaction on Pt catalysts. On Ir on the other hand, NO formation is more difficult. This difference is most clearly seen when the surface composition and gas phase products are measured during temperature programmed reaction, as is done in this study and also in, for example, Refs. [8,26]. On Pt, the surface composition is directly reflected in the gas phase product distribution: a surface predominantly covered with N_{ad} produces mainly N_2, an O_{ad}-covered surface produces NO [26]. On Ir the surface composition and gas phase selectivity change are not synchronized, and temperature differences of 80 K [Ir(1 1 1)] up to 200 K [Ir(1 1 0)] have been found.

The formation rate of N_2 and NO as a function of surface coverage and temperature can in first approximation be described with the kinetic expressions shown in equations 4 and 5, in which k_{N_2} and k_{NO} represent the rate constants for N_2 and NO formation, and θ_N and θ_O represent the coverage of N_{ad} and O_{ad}:

$$\frac{d[N_2]}{dt} = k_{N_2}\theta_N^2 \quad (4)$$

$$\frac{d[NO]}{dt} = k_{NO}\theta_N\theta_O \quad (5)$$

The experimental observations show that the NO formation rate on Ir(1 1 1) does not depend directly on θ_N and θ_O. This means that the selectivity is determined by a difference between k_{N_2} and k_{NO}, i.e. the activation energy of N_2 formation should be significantly lower than that of NO formation. We have constructed an energy scheme (Fig. 5) for N_2 and NO formation on Ir(1 1 1) and Pt(1 1 1) by using theoretically predicted values from literature [37,38]. Both studies were performed by the same group, and a very similar approach was used for both surfaces. We used the adsorption energies obtained with the PW91 functional to produce the figure. The activation energies were calculated from the adsorption energies of the atomic reactants using the Brønsted–Evans–Polanyi relationship [39,40] from the work of Nørskov et al. [41].

From this figure the difference between Pt and Ir becomes clear. The barriers for N_2 formation on both surfaces are around ~200 kJ mol^{-1}. More importantly, the transition state energy lies above the energy of the N_2 molecule in the gas phase. This means that the N_2 molecule will immediately desorb upon formation and the experimentally observed barrier is equal to the barrier height for N_2 formation. For NO formation the situation is different. The activation barrier to form the NO molecule is ~20 kJ mol^{-1} higher than to form N_2 and it is similar both on Pt and Ir. For Pt the energy of the transition state is above that of NO (g), i.e., NO will desorb upon formation, and the experimentally observed activation energy is equal to the barrier height. On Ir, on the other hand, the energy of the transition state is *below* that of NO (g), meaning that additional

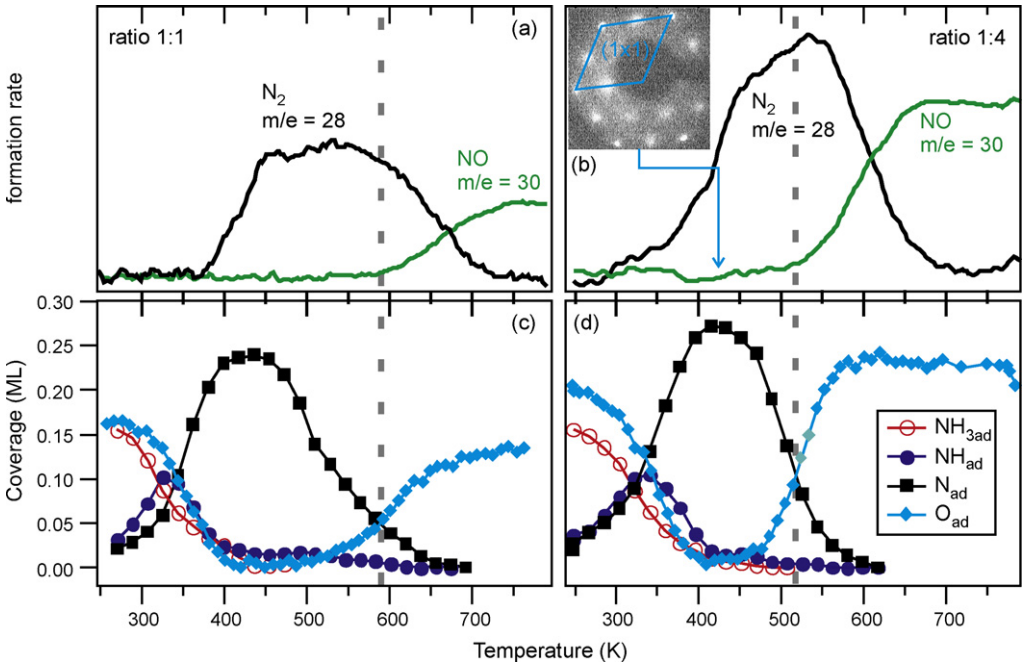

Fig. 4. Temperature programmed reaction (TPR, 0.7 K s^{-1}) and TP-XPS (0.4 K s^{-1}) during ammonia oxidation, for two reactant ratios. The NH_3 pressure was kept constant at 5×10^{-8} mbar during the TP-XPS, while for the TPR data a constant NH_3 pressure of 5×10^{-7} mbar was used. The O_2 pressure was adjusted according to the desired ratio. For both ratios, the surface coverage changes from N_{ad} to O_{ad}, but the selectivity change in the gas phase from N_2 to NO is shifted by 80 K to higher temperatures.

energy (30 kJ mol^{-1}) is needed to desorb the NO molecule in the gas phase. The result is that the barrier for NO (g) formation on Pt is only ~20 kJ mol^{-1} higher than that of N_2 formation, whereas on Ir(1 1 1) it is ~50 kJ mol^{-1} higher. The reason behind this difference is the much stronger adsorption of the atomic species on Ir as compared to Pt. This explains the stronger preference for N_2 formation on Ir(1 1 1).

The shift of the NO formation to lower temperatures with increasing O_2 partial pressure can be explained by coverage effect which are not present in the ideal theoretical model. We offer here two different explanations, which could both play a role: (i) the O_{ad} concentration reaches higher values for higher O_2 partial pressures. As a result the O_{ad} adsorption energy decreases, which means that energy of the reactants and the transition state shifts upward, bringing the transition state closer to that of NO (g), thus lowering the barrier for NO (g) formation. (ii) An alternative explanation can be directly derived from the energy scheme in Fig. 5. The formation of NO_{ad} becomes feasible at higher temperature, but it is endothermic, so the equilibrium is shifted toward the side of the atomic adsorbates. A high concentration of O_{ad} can inhibit NO dissociation, and the NO_{ad} that is formed desorbs rather than dissociates.

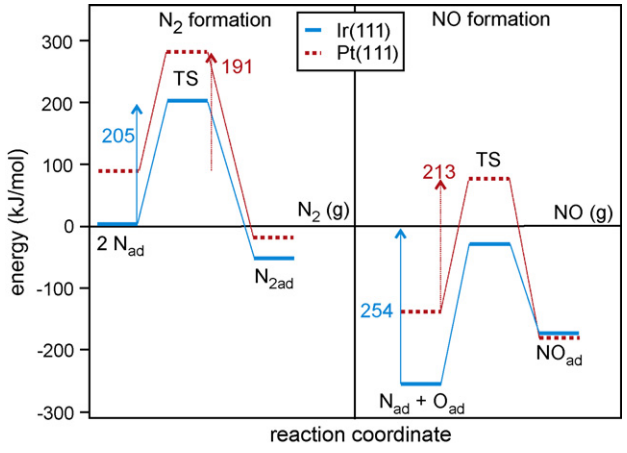

Fig. 5. Schematic energy diagram for N_2 and NO formation on Pt(1 1 1) and Ir(1 1 1). The values for Ir(1 1 1) were adapted from Ref. [37]. The values for Pt(1 1 1) were adapted from Ref. [38]. The experimentally relevant barriers included in the figure.

4. Summary and conclusions

The NH_3 surface chemistry on Ir(1 1 1) has been studied using XPS and desorption measurements. NH_3 does not dissociate on Ir(1 1 1), but radiation can induce dissociation. On a beam-damaged sample at low temperature a mixture of NH_{3ad}, NH_{2ad}, NH_{ad} and N_{ad} is found, but N_{ad} and NH_{2ad} converted below 300 K to NH_{ad}, which was found to be the most stable NH_{xad} surface species. It decomposes between 400 and 500 K, during which N_{ad}, N_2, NH_3 (g) and some H_2 are formed, in a complex interplay between NH_{ad} decomposition, NH_{ad} hydrogenation, and H_2 desorption.

The presence of O_{ad} enables NH_3 dissociation at low temperature, forming NH_{ad} between 280 and 400 K. Atomic oxygen also destabilizes NH_{ad}, which reacts with O_{ad} to N_{ad} above 350 K (instead of 400 K found in the absence of O_{ad}). The formation of NO_{ad} or NO (g) was not observed, in contrast to findings on Ir(1 1 0), where NO_{ad} was formed above 400 K.

During temperature programmed ammonia oxidation the surface composition below 500 K is dominated by N_{ad}, above 500 K the surface composition changes and O_{ad} is the only adsorbate present in measurable quantities above 650 K. The temperature at which the surface composition changes depends on the exact NH_3/O_2 reactant ratio. The gas phase selectivity also shifts, from N_2 to NO, but this occurs ~80 K higher than the change of surface composition. This finding is explained by looking at the barriers for N_2 vs. NO formation on Ir(1 1 1). The strong adsorption of atomic adsorbates on Ir(1 1 1) gives rise to a barrier that is 50 kJ mol^{-1} higher than that of N_2 formation on the same surface. On Pt(1 1 1) the adsorption of atomic adsorbates is weaker, and the barriers for NO and N_2 formation differ by only 20 kJ mol^{-1}.

Acknowledgements

The authors acknowledge ELETTRA and the European Union for financial support to perform measurements at the SuperESCA beamline of ELETTRA. S. Lizzit, L. Petaccia and A. Baraldi are acknowledged for their help during the beamtime. C.J.W. acknowledges the Netherlands Technology foundation STW, the applied science division of NWO and the technology programme of the Ministry of Economic Affairs, for financial support under project number UPC.5037.

Appendix A. Supplementary data

Supplementary data associated with this article can be found, in the online version, at doi:10.1016/j.cattod.2010.03.049.

References

[1] A.C.M. van den Broek, J. van Grondelle, R.A. van Santen, J. Catal. 185 (1999) 297–306.
[2] T.V. Choudhary, A.K. Santra, C. Sivadinaranaya, B.K. Min, C.W. Yi, K. Davis, D.W. Goodman, Catal. Lett. 77 (1–3) (2001) 1–5.
[3] A.K. Santra, B.K. Min, C.W. Yi, K. Luo, T.V. Choudhary, D.W. Goodman, J. Phys. Chem. B 106 (2002) 340–344.
[4] S.A.C. Carabineiro, B.E. Nieuwenhuys, Surf. Sci. 505 (2002) 163–170.
[5] S.A.C. Carabineiro, B.E. Nieuwenhuys, Surf. Sci. 532 (2003) 87–95.
[6] C.J. Weststrate, J.W. Bakker, E.D.L. Rienks, S. Lizzit, L. Petaccia, A. Baraldi, C.P. Vinod, B.E. Nieuwenhuys, J. Chem. Phys. 122 (18) (2005) 184705.
[7] C.J. Weststrate, J.W. Bakker, E.D.L. Rienks, S. Lizzit, L. Petaccia, A. Baraldi, C.P. Vinod, B.E. Nieuwenhuys, Phys. Chem. Chem. Phys. 7 (13) (2005) 2629–2634.
[8] C.J. Weststrate, J.W. Bakker, E.D.L. Rienks, J.R. Martinez, S. Lizzit, L. Petaccia, A. Baraldi, C.P. Vinod, B.E. Nieuwenhuys, J. Catal. 235 (1) (2005) 92–102.
[9] C.A. de Wolf, J.W. Bakker, P.T. Wouda, B.E. Nieuwenhuys, A. Baraldi, S. Lizzit, M. Kiskinova, J. Phys. Chem. B 105 (2001) 4254–4262.
[10] W.D. Mieher, W. Ho, Surf. Sci. 322 (1995) 151–167.
[11] A.F. Carley, P.R. Davies, M.W. Roberts, Chem. Commun. 185 (1998) 1793–1794.
[12] S.A.C. Carabineiro, A.V. Matveev, V.V. Gorodetskii, B.E. Nieuwenhuys, Surf. Sci. 555 (2004) 83–93.
[13] A.L. Schwaner, E.D. Pylant, J.M. White, J. Vac. Sci. Technol. A 14 (3) (1996) 1453–1456.
[14] H. Guo, D. Chrysostomou, J. Flowers, F. Zaera, J. Phys. Chem. B 107 (2003) 502–511.
[15] R.M. van Hardeveld, R.A. van Santen, J.W. Niemantsverdriet, Surf. Sci. 369 (1996) 23–35.
[16] T.H. Chilton, The Manufacture of Nitric Acid by the Oxidation of Ammonia, Monograph Series No. 3, American Institute of Chemical Engineers, New York, 1960.
[17] J.J. Joyce, M. del Guidice, J.H. Weaver, J. Electron Spectrosc. Relat. Phenom. 49 (1) (1989) 31–45.
[18] P.A. Zhdan, G.K. Boreskov, A.I. Boronin, W.F. Egelhoff, W.H. Weinberg, Surf. Sci. 61 (1976) 25–36.
[19] J.C.L. Cornish, N.R. Avery, Surf. Sci. 235 (1990) 209–216.
[20] C.M. Chan, W.H. Weinberg, J. Chem. Phys. 71 (7) (1979) 2788–2792.
[21] D.I. Hagen, B.E. Nieuwenhuys, G. Rovida, G.A. Somorjai, Surf. Sci. 57 (1976) 632.
[22] M. Bianchi, D. Cassese, A. Cavallin, R. Comin, F. Orlando, L. Postregna, E. Golfetto, S. Lizzit, A. Baraldi, New J. Phys. 11 (2009) 063002.
[23] R.J. Purtell, R.P. Merrill, C.W. Seabury, T.N. Rhodin, Phys. Rev. Lett. 44 (19) (1980) 1279–1281.
[24] Y.-M. Sun, D. Sloan, H. Ihm, J.M. White, J. Vac. Sci. Technol. A 14 (3) (1996) 1516–1521.
[25] E. Herceg, K. Mudiyanselage, M. Trenary, J. Phys. Chem. B 109 (2005) 2828–2835.
[26] C.J. Weststrate, J.W. Bakker, E.D.L. Rienks, C.P. Vinod, A.V. Matveev, V.V. Gorodetskii, B.E. Nieuwenhuys, J. Catal. 242 (2006) 184–194.
[27] C.A. de Wolf, J.W. Bakker, P.T. Wouda, B.E. Nieuwenhuys, A. Baraldi, S. Lizzit, M. Kiskinova, J. Chem. Phys. 113 (2000) 10717–10722.
[28] C.J. Hagedorn, M.J. Weiss, W.H. Weinberg, Phys. Rev. B 60 (1999) R14016.
[29] E.S. Kurkina, N.L. Semendyaeva, A.I. Boronin, Kinet. Catal. 42 (5) (2001) 703–717.
[30] B. Hammer, J.K. Nørskov, Surf. Sci. (1995) 211–220.
[31] W.K. Offermans, A.P.J. Jansen, R.A. van Santen, Surf. Sci. 600 (2006) 1714–1734.
[32] J.M. Gohndrone, C.W. Olsen, A.L. Backman, T.R. Gow, E. Yagasaki, R.I. Masel, Ammonia adsorption and decomposition on several faces of platinum, J. Vac. Sci. Technol. A 7 (3) (1989) 1986–1990.
[33] J.J. Vajo, W. Tsai, W.H. Weinberg, J. Phys. Chem. 89 (1985) 3243–3251.
[34] J.L. Gland, E.B. Kollin, Surf. Sci. 104 (1981) 478–490.
[35] J.M. Bradley, A. Hopkinson, D. King, Surf. Sci. 371 (1997) 255–263.
[36] M. Kim, S.J. Pratt, D.A. King, J. Am. Chem. Soc. 122 (2000) 2409–2410.
[37] W.P. Krekelberg, J. Greeley, M. Mavrikakis, J. Phys. Chem. B 108 (2004) 987–994.
[38] M.M. Denise, C. Ford, Y. Xu, Surf. Sci. 587 (2005) 159–174.
[39] N. Brønsted, Chem. Rev. 5 (1928) 231.
[40] M.G. Evans, N.P. Polanyi, Trans. Faraday Soc. 34 (1938) 11.
[41] J.K. Nørskov, T. Bligaard, A. Logadottir, S. Bahn, L.B. Hansen, M. Bollinger, H. Bengaard, B. Hammer, Z. Sljivancanin, M. Mavrikakis, Y. Xu, S. Dahl, C.J.H. Jacobsen, J. Catal. 209 (2002) 275–278.